

## Thiết kế anten PIFA băng tần kép nhỏ gọn cho hệ thống thông tin 5G

Huỳnh Nguyễn Bảo Phương\*, Đặng Thị Từ Mỹ

*Khoa Kỹ thuật & Công nghệ, Trường Đại học Quy Nhơn, Việt Nam*

*Ngày nhận bài: 26/04/2023; Ngày nhận đăng: 08/06/2023; Ngày xuất bản: 28/06/2023*

### TÓM TẮT

Bài báo này đề xuất một anten PIFA băng tần kép hoạt động ở tần số 28/38 GHz cho hệ thống thông tin 5G. Anten PIFA gồm 2 lớp điện môi với một lớp không khí ở giữa. Cả hai lớp điện môi đều là Roger RT có hệ số điện môi tương đối là 2,2 và độ dày là 0,127 mm. Tấm bức xạ của anten là một miếng vá hình chữ nhật được khoét một khe xoắn ốc trên bề mặt để tạo ra băng tần kép tại 28 GHz và 38 GHz. Ban đầu, anten đề xuất được thiết kế dựa trên tính toán lý thuyết và sau đó được tối ưu kết quả bằng mô phỏng số sử dụng Phương pháp phần tử hữu hạn (FEM). Chiều dài tổng của tấm bức xạ xấp xỉ  $0.25\lambda_g$  tại tần số 28 GHz. Kết quả mô phỏng số cho thấy anten PIFA đề xuất có thể hoạt động ở băng tần kép với dài phôi hợp trở kháng đạt 5,7% (27 - 28,6 GHz) với  $|S11| \leq -10$  dB và hệ số tăng ích thực đạt 6,81 dBi tại tần số cộng hưởng thứ nhất 28 GHz và dài phôi hợp trở kháng đạt 14,5% (35,7 - 41,2 GHz) với  $|S11| \leq -10$  dB và hệ số tăng ích thực đạt 6,81 dBi tại tần số cộng hưởng thứ nhất 28 GHz.

**Từ khóa:** *Anten PIFA, băng tần kép, hệ thống thông tin 5G.*

\*Tác giả liên hệ chính.

Email: *huynhnguyenbaophuong@qnu.edu.vn*

# Design of Compact Dual-band PIFA Antenna for 5G Communication Systems

Huynh Nguyen Bao Phuong\*, Dang Thi Tu My

*Faculty of Engineering and Technology, Quy Nhon University, Vietnam*

*Received: 26/04/2023; Accepted: 08/06/2023; Published: 28/06/2023*

## ABSTRACT

This paper proposes a dual-band PIFA antenna operated at 28/38 GHz for 5G communication systems. The PIFA antenna consists of two dielectric layers and an air gap is inserted between these two layers. Both substrates, namely Roger RT dielectric, have a relative dielectric constant of 2.2 and a thickness of 0.127 mm. The radiator of the antenna is a rectangular patch in which a spiral slot is etched on its surface to create dual-band frequencies of 28 GHz and 38 GHz. Firstly, the proposed antenna is designed based on the theoretical calculations and then the numerical simulation using Finite Element Method (FEM) is used to optimize results. The total length of the radiator is approximately  $0.25\lambda_g$  at the frequency of 28 GHz. The numerical results indicated the proposed PIFA antenna can be operated in a dual-band frequency with an impedance matching of 5.7 % (27 - 28.6 GHz) for  $|S11| \leq -10$  dB and a realized gain up to 6.81 dBi for the first resonant frequency at 28 GHz and an impedance matching of 14.5% (35.7 - 41.2 GHz) for  $|S11| < -10$  dB and a realized gain up to 7.92 dBi for the second resonant one.

**Keywords:** *Dual-band, PIFA antenna, 5G communication systems.*

## 1. INTRODUCTION

Developing the compact antenna for 5G communication system has become an emerging interest among researchers due to the requirement of millimeter wave (mmW) systems in high-speed data and integration ability in a mobile device.<sup>1</sup> Up to now, the lower frequencies (below 6 GHz) have been used widely for 5G technology, while the higher one for mmW applications are still being researched and developed.<sup>2</sup> Given the advantages on wide band and the ability to provide high data rate, the upcoming use of the mmW band, i.e, 5G systems at 28 and 38 GHz frequencies increasingly attracts the interest of many researchers, especially the antenna for 5G systems.<sup>3-6</sup>

The PIFA antennas with the frequency bands of sub-6 GHz is popularly used in cell phones and other RF devices. Due to the unique characteristic in electrically small size of a quarter wavelength antenna, the PIFA antennas can be applied to integrate into 5G systems when the frequency bands reach 28 and 38 GHz. Thus, the wireless systems can transmit in different bands by using one antenna. The application of one antenna in wireless systems can minimize the communication systems.<sup>7-13</sup>

A dual-band PIFA antenna was investigated in the previous study of Hashem et al.<sup>14</sup> In this study, the antenna included a metallic patch connected to the ground plane by shorted pin with an air substrate. The system was operated

---

\*Corresponding author:

Email: [huynhnguyenbaophuong@qnu.edu.vn](mailto:huynhnguyenbaophuong@qnu.edu.vn)

at 28 GHz and 38 GHz with a form factor of (1.3 mm x 1.83 mm). As a result, a quite high gain of 5 dBi and 5.5 dBi at the frequency of 28 GHz and 38 GHz, respectively was observed.<sup>14</sup> However, this antenna still has some disadvantages related to bandwidths. The narrow bandwidths of 700 MHz and 300 MHz were measured at 28 GHz and 38 GHz, respectively. After few years, a wide dual-band PIFA antenna with a small form factor had been proposed.<sup>1</sup> However, this antenna did not reach good performances at 28 GHz and 38 GHz. For instance, peak gain was only 3.75 dBi and 5.06 dBi.

This study aims to propose and investigate a dual-band PIFA antenna on double substrates with a small overall size. To increase the impedance bandwidths, an air layer was inserted into the two dielectric layers. As a result, the proposed PIFA yields a wide bandwidth and a high realized gain at both frequencies.

## 2. SINGLE-BAND PIFA ANTENNA DESIGN

There are three parts in this section. Firstly, the model of the single band PIFA antenna is proposed. After that, all the dimensions of the proposed PIFA are theoretically calculated based on the desired resonant frequency. Finally, the ANSYS Academic Research HF is used to simulate and optimize the initial dimensions for getting the final design.

### 2.1. Antenna geometry

The proposed PIFA antenna consists of two Roger RT dielectric layers with the same relative dielectric constant ( $\epsilon_r$ ) of 2.2 and a thickness ( $H_s$ ) of 0.127 mm. A rectangular radiator metal plate ( $W \times L$ ) (mm<sup>2</sup>) is placed on the first dielectric layer. This plate is connected to a metallic ground plane by a metallic via. The second dielectric layer is put on the ground plane. An air layer with a thickness ( $H_{air}$ ) of 0.344 mm is inserted between the two dielectric layers. The antenna is fed by a coaxial with an impedance of 50  $\Omega$ . The proposed PIFA antenna's configuration is depicted in Figure 1.

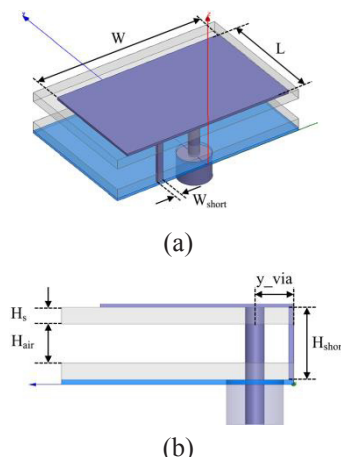


**Figure 1.** Configuration of the proposed single PIFA antenna: (a) Perspective view, (b) Side view.

### 2.2. Theoretical calculation

Based on microstrip antenna theory, the PIFA resonances at the frequency corresponding to the antenna's length is equal to  $\frac{1}{4}$  wavelength at its resonant frequency.<sup>15</sup>

$$(L + W - W_{short})\sqrt{\epsilon_{eff}} \approx \frac{\lambda}{4} \quad (1)$$

$$f = \frac{c}{4(L + W - W_{short})\sqrt{\epsilon_{eff}}} \quad (2)$$

$$\text{where, } \epsilon_{eff} = \frac{\epsilon_r \cdot \epsilon_{air} (H_s + H_{air})}{\epsilon_r \cdot H_{air} + \epsilon_{air} \cdot H_s} \quad (3)$$

The effective dielectric constant ( $\epsilon_{eff}$ ) is calculated:

$$\epsilon_{eff} = \frac{2.2 \times 1(0.127 + 0.354)}{2.2 \times 0.354 + 1 \times 0.127} \approx 1.17$$

The radiator size of the antenna at 28 GHz is calculated as Eq. (2). Thus, the initial dimensions of the antenna are chosen as follows:  $L = 1.1$  mm,  $W = 1.32$  mm và  $W_{short} = 0.05$  mm. The calculated results of the proposed antenna are provided in Table 1.

**Table 1.** Theoretical calculation dimensions of the proposed PIFA antenna (unit: mm).

Parameter	Value	Parameter	Value
W	1.32	L	1.1
W <sub>g</sub>	1.52	L <sub>g</sub>	1.3
W <sub>short</sub>	0.05	H <sub>short</sub>	0.55

### 2.3. Simulation and optimization

Return loss simulated result of the PIFA with the initial dimensions is depicted in Figure 2. It can be seen that the proposed single band PIFA yields a center frequency of 29.2 GHz. This simulated frequency is quite close to the one of theoretical calculation and it will be optimized to obtain the desired frequency of 28 GHz by investigating the dimensions of the antenna.

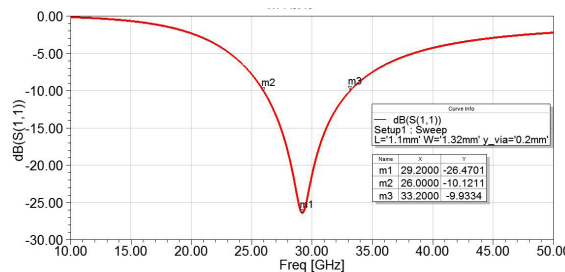


**Figure 2.** Simulated S11 of the PIFA with its theoretical calculation dimensions.

In order to determine the optimal dimensions corresponding to the desired resonant frequency at 28 GHz, the length ( $L$ ) and the width ( $W$ ) of the PIFA are selected for investigation. One parameter will be changed for investigating while another one will be fixed. Firstly, the width of the rectangular patch is considered when the length is fixed at 1mm. The simulation reflection coefficient of the PIFA with various values of  $W$  is shown in Figure 3. It is observed that the resonant frequency of the antenna decreases as the width of its radiator increases or the total electrical length of the proposed antenna increases. This observation is consistent with the theory when the frequency of the antenna its electrical length is inversely proportional each other, as shown in Eq. (2).

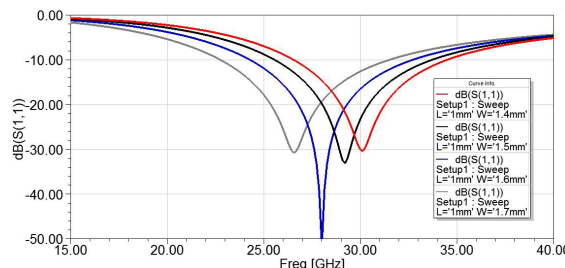


**Figure 3.** Simulated S11 of the single band antenna versus various values of  $W$ .

Next, the length of the patch ( $L$ ) is investigated when the width  $W$  is set at 1.4 mm. Numerical S11 results of the antenna with various values of  $L$  are shown in Figure 4. Similarly, increasing the patch length leads to decrease the resonant frequency. These results could be explained that when the length of the patch changes, the electrical length of the antenna changes, which leads to the change in the resonant frequency.

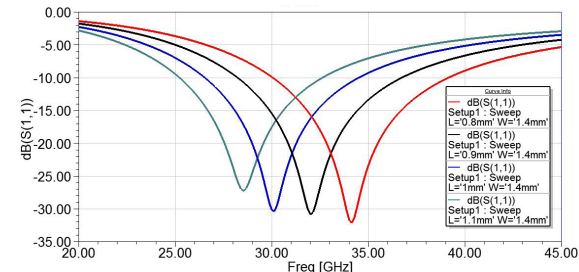


**Figure 4.** Simulation results of S11 of the single band PIFA with the various values of  $L$ .

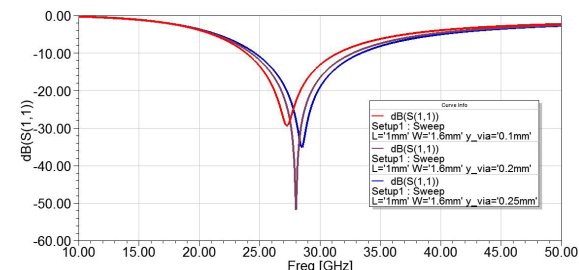


**Figure 5.** Simulation results of S11 of the single antenna versus to different values of  $y_{via}$ .

After adjusting  $W$  and  $L$  to optimize the center frequency of the PIFA at 30 GHz, the position of feeding will be considered for optimizing the impedance matching. This optimization is utilized by changing the value of  $y_{via}$ . The reflection coefficient simulated of the antenna with different values of the antenna's feeding positions ( $y_{via}$ ) is presented in Figure 5. This observation shows that the impedance matching's antenna changes as the  $y_{via}$  value changes. In particular, when the value of  $y_{via}$  changed from 0.1 to 0.25 mm the antenna exhibits the best impedance matching as  $y_{via}$  is equal to 0.2 mm. The impedance of the rectangular patch antenna will be maximum at its edge and be zero at its center. Thus, the change in feeding leads to

the change in antenna impedance. The optimal dimensions of the proposed single antenna at 28 GHz are presented in Table 2.

**Table 2.** Optimal dimensions of the single band PIFA (unit: mm).

Parameter	Value	Parameter	Value
W	1.6	L	1.1
W <sub>g</sub>	1.8	L <sub>g</sub>	1.3
W <sub>short</sub>	0.05	H <sub>short</sub>	0.598
x_via	0	y_via	0.2

The simulation result of S11 at the final single antenna are depicted in Figure 6. As can be observed, the final PIFA yields a center frequency of 28 GHz with -10 dB bandwidth spreading from 24.26 to 32.66 GHz. In particular, the proposed antenna exhibits a very good impedance matching of -51.8 dB.

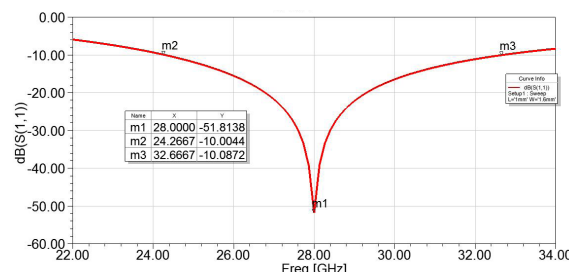


**Figure 6.** Simulated S11 of the final single antenna.

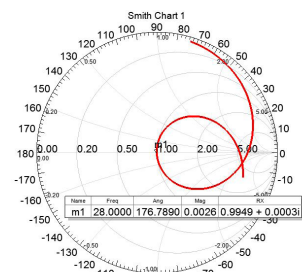


**Figure 7.** Simulated input impedance of the final antenna at 28 GHz.

To validate the impedance matching ability between  $50 \Omega$  feeder and the antenna, the impedance simulation is realized in the Smith chart, as shown in Figure 7. It can be seen at 28 GHz (the point of m1) that the antenna has a normalized input impedance of 0.9949 at the real part and approximately 0 at the imaginary part. The actual impedance of the antenna is approximately  $50 \Omega$  ( $0.9949 \times 50$ ). Thus, the

above results demonstrated that the final antenna yields a perfect impedance matching.

The simulated radiation pattern of the final antenna at 28 GHz is exhibited in Figure 8. It is clear that the antenna exhibits a directional in the E-plane (Solid line) with a peak gain of 6.9 dBi.

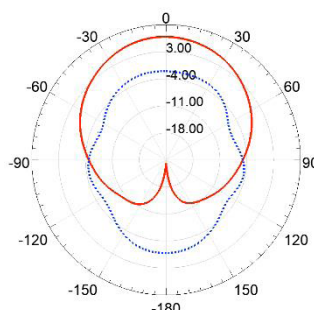


**Figure 8.** Simulated radiation pattern of the single antenna at 28 GHz.

The current distribution of the antenna at 28 GHz is shown in Figure 9. The current is almost focused on the edges of the rectangular patch.

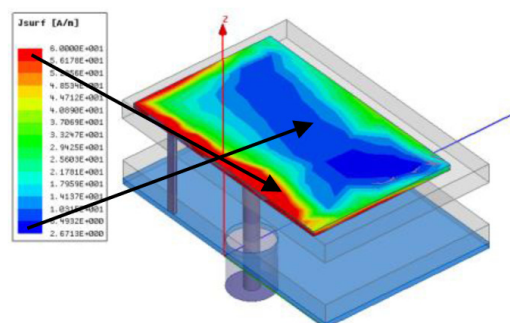


**Figure 9.** Current distribution on antenna surface at 28 GHz.

### 3. DUAL-BAND PIFA ANTENNA DESIGN

In this section, the dual-band PIFA was designed based on the proposed single one. A spiral slot is cut on the rectangular patch of the single antenna to produce the second resonant mode.

#### 3.1. Antenna geometry

The dual-band PIFA antenna is built based on the design of the single-band antenna in Section 2 with a spiral etched slot on the surface of the patch. This method aims to create the second resonance at 38 GHz. The configuration of the dual-band PIFA is shown in Figure 10. The spiral slot consists of five straight slots and its total length is the sum of the length of five straight slots.

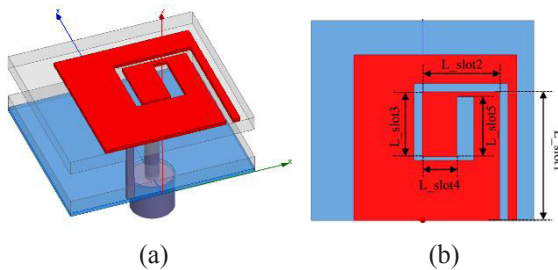


**Figure 10.** Geometry of the proposed dual-band PIFA: (a) Perspective view, (b) Top view.

### 3.2. Theoretical calculation

The spiral slot length ( $L_{slot}$ ) corresponding to the resonance of 38 GHz is calculated as follows<sup>15</sup>:

$$f = \frac{c}{4L_{slot}\sqrt{\epsilon_{eff}}} \quad (4)$$

$$L_{slot} = \frac{c}{4f\sqrt{\epsilon_{eff}}} = \frac{3 \cdot 10^8}{4 \cdot 38 \cdot 10^9 \sqrt{1,17}} = 1,82 \text{ mm}$$

Where,

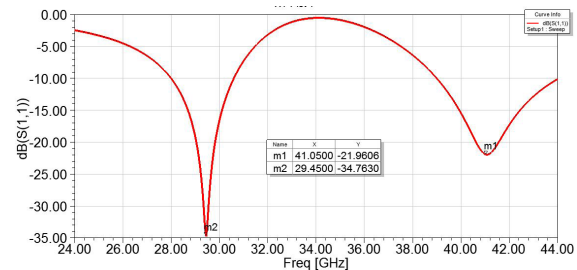
$$L_{slot} = L_{slot1} + L_{slot2} + L_{slot3} + L_{slot4} + L_{slot5}$$

From the value of  $L_{slot}$ , the initial length of the straight slots was easily chosen:  $L_{slot1} = 0,75 \text{ mm}$ ;  $L_{slot2} = 0,45 \text{ mm}$ ;  $L_{slot3} = 0,38 \text{ mm}$ ;  $L_{slot4} = 0,2 \text{ mm}$ , and  $L_{slot5} = 0,1 \text{ mm}$ .

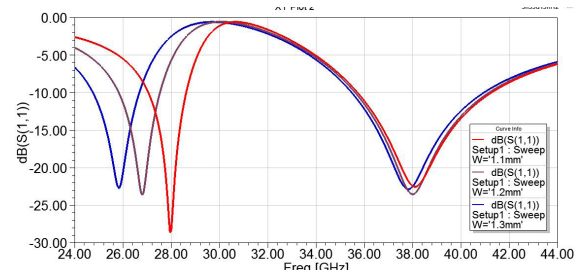
### 3.3. Simulation and optimization

Figure 11 depicts the simulated reflection coefficient of the dual-band PIFA as its theoretical calculated dimensions. As can be observed from this figure, the PIFA antenna yields a dual-band performance with the lower frequency at 29.45 GHz and the higher frequency at 41.05 GHz. From these calculated frequencies, the dimensions of the initial dual-band PIFA was optimized to reach the final design of the dual-band antenna operated at the frequency of 28 and 38 GHz.

The dimensions of the dual-band antenna were justified to verify with the center frequencies of both bands. From that, the length and the width of the rectangular patch and the slot were investigated with different values. This method aims to find out the optimal values in which the PIFA antenna was operated at two center frequencies of 28 and 38 GHz.



**Figure 11.** Simulated S11 of the dual-band PIFA as the theoretical calculation.



**Figure 12.** Simulated S11 of the dual-band antenna versus various values of W.

Figure 12 depicts the simulated S11 results with various values of the patch width while the other dimensions are fixed. As can be observed in Figure 12, increasing the patch width led to decreasing the lower frequency. Meanwhile, the higher one is not hardly change. It is noted that when the width ( $W$ ) of rectangular patch increased, the total length of the antenna also increased. Therefore, the lower resonance was decreased since it is inversely proportional to the antenna's total length.

Return loss simulated versus various values of patch length ( $L$ ) is shown in Figure 13. Two frequencies decreased as the patch length increased. This result is well consistent with the theory since the resonant frequency of the antenna is inversely proportional to its length.

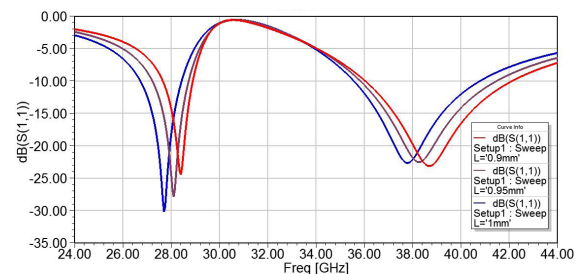


**Figure 13.** Simulated S11 versus different values of L.

The length ( $L_{slot5}$ ) and the width ( $H_{slot5}$ ) of the fifth slot were used for optimizing the desired frequencies. Figure 14 shows the reflection coefficient simulated results of the dual-band antenna with different values of  $L_{slot5}$ . The width and the length of the patch are fixed at 1.1 mm and 0.95 mm, respectively. The simulated  $S_{11}$  of the antenna versus various values of  $H_{slot5}$  is indicated in Figure 15. The value of  $L_{slot5}$  was set at 0.35 mm, and the values of  $W$  and  $L$  were also fixed as mentioned in the simulation scenario in Figure 14. The simulated results presented in Figure 14 and 15 show that the two centre frequencies decrease while the two values decrease.

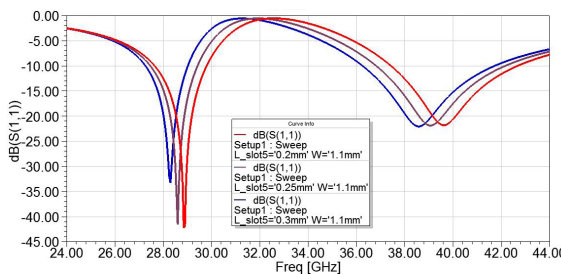


**Figure 14.** Simulated  $S_{11}$  of the antenna versus different values of  $L_{slot5}$ .

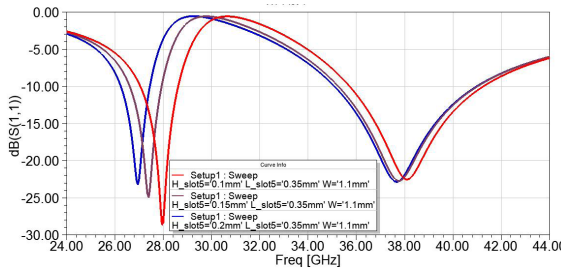


**Figure 15.** Simulated  $S_{11}$  of the antenna versus different values of  $H_{slot5}$ .

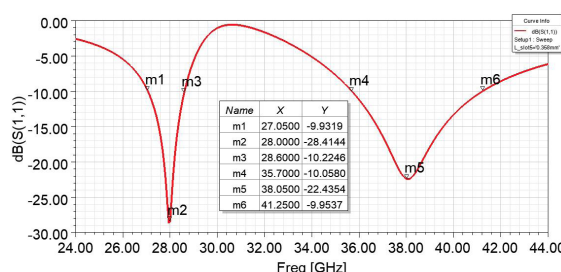


**Figure 16.** Simulated  $S_{11}$  of final dual-band PIFA at 28 GHz and 38 GHz.

**Table 3.** Optimal dimensions of the dual-band PIFA (unit: mm).

Parameter	Value	Parameter	Value
$W$	1,1	$L_{slot2}$	0,45
$L$	0,965	$L_{slot3}$	0,38
$W_g$	1,8	$L_{slot4}$	0,2
$L_g$	1,3	$L_{slot5}$	0,35
$W_{short}$	0,05	$H_{slot1}$	0,05
$H_{short}$	0,598	$H_{slot2}$	0,05
$x_{via}$	0	$H_{slot3}$	0,06
$y_{via}$	0,2	$H_{slot4}$	0,02
$L_{slot1}$	0,75	$H_{slot5}$	0,1

The simulated  $S_{11}$  of the dual-band antenna at the final design is exhibited in Figure 16. The final PIFA yields dual-band resonances operated at the centre frequencies of 28 and 38 GHz corresponding to the -10 dB bandwidth of 1.53 and 5.53 GHz. The optimal dimensions corresponding to the final design are illustrated in Table 3.

In order to verify the effect of the slot to the radiation of the proposed dual-band PIFA, the current distribution in the numerical simulation is shown in Figure 17. The current distribution at 28 and 38 GHz was different. The current distribution at 28 GHz concentrated at the outside edges of the slot whereas that at 38 GHz focused on the inside edges of the slot.

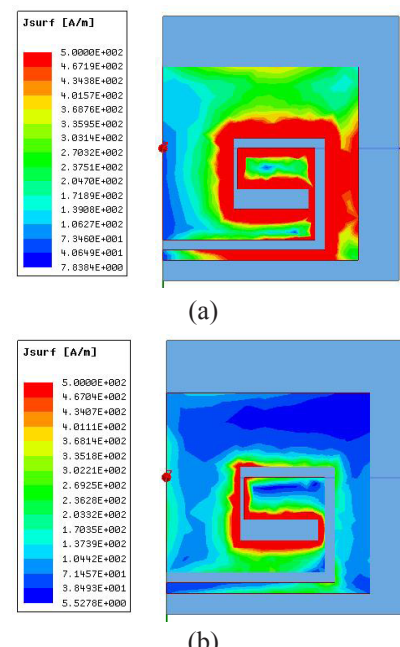


**Figure 17.** Current distribution on the dual-band PIFA antenna at: (a) 28 GHz, (b) 38 GHz.

Figure 18 shows the simulation result of the radiation pattern of the final dual-band antenna at 28 and 38 GHz. The solid curve is represented for E plane while the dash one is represented for H plane. From this figure, the antenna exhibits a directional pattern in xz plane with the realized gain at 28 GHz and 38 GHz is 6.81 dBi and 7.92 dBi, respectively.

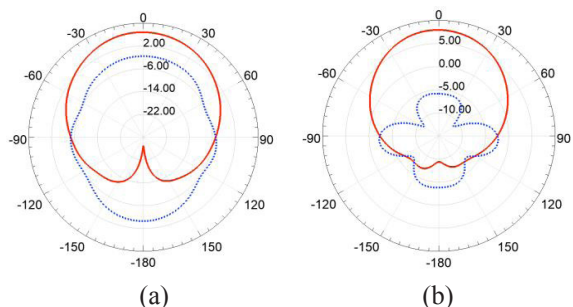


**Figure 18.** Simulated radiation pattern of the final dual-band antenna at: (a) 28 GHz, (b) 38 GHz.

Table 4 presents the comparison between the proposed PIFA and the other PIFA antennas reported in literature.<sup>1,12,14</sup> The proposed dual-band PIFA in this study exhibits good radiation characteristics in terms of -10 dB bandwidth and realized gain as well as the smallest form factor in comparison to the listed studies.

**Table 4.** Comparison between the proposed dual-band PIFA with the reported PIFA in literature.

Ref.	Overall size (mm×mm×mm)	Bandwidth (GHz)		Gain (dBi)	
		28 GHz	38 GHz	28 GHz	38 GHz
1	3×7×1.2	3.34	1.39	3.75	5.06
12	3.8×5.5×0.381	0.7	0.3	5	5.5
16	4×5.5×0.2	0.89	0.99	6.22	6.33
This work	1.3×1.8×0.598	1.53	5.53	6.81	7.92

#### 4. CONCLUSION

A dual-band PIFA antenna for 5G communication systems has been designed, simulated and optimized in this study. The proposed PIFA consists of two dielectric layers and an air layer inserted between these two layers. Based on the PIFA antenna operated at 28 GHz, a spiral slot is

etched on the patch radiator to create the second resonance at 38 GHz. Based on the initial results obtained by the theoretical calculation, the proposed PIFA antenna is optimized to achieve a dual-band resonances centred at the frequency of 28 GHz and 38 GHz. The antenna exhibits good performances with wide -10 dB bandwidth of 1.53 GHz and 5.53 GHz and the realized gain of 6.81 dBi and 7.92 dBi corresponding to 28 GHz and 38 GHz. The proposed antenna can be applied for 5G communication systems.

#### REFERENCES

1. W. Ahmad and W. T. Khan. Small form factor dual-band (28/38 GHz) PIFA antenna for 5G applications, *Proceedings of the IEEE MTT-S International Conference on Microwaves for Intelligent Mobility (ICMIM)*, 2017.
2. C. Han, Y. Bi, S. Duan, and G. Lu. Rain rate retrieval test from 25-ghz, 28-ghz, and 38-ghz millimeter-wave link measurement in Beijing, *IEEE Journal of Selected Topics in Applied Earth Observations and Remote Sensing*, **2019**, 12(8), 2835-2847.
3. H. M. Marzouk, I. A. Mohamed, and H. A. S. Abdel. Novel dual-band 28/38 GHz MIMO antennas for 5G mobile applications, *Progress In Electromagnetics Research C*, **2019**, 93, 103-117.
4. N. Ashraf, O. Haraz, M. A. Ashraf, and S. Alshebeili. *28/38-GHz dual-band millimeter wave SIW array antenna with EBG structures for 5G applications*, *Proceedings of the International Conference on Information and Communication Technology Research (ICTRC)*, 2015.
5. T. Deckmyn, M. Cauwe, D. V. Ginste, H. Rogier, and S. Agneessens. Dual-Band (28,38) GHz coupled quarter-mode substrate-integrated waveguide antenna array for next-generation wireless systems, *IEEE Transactions on Antennas and Propagation*, **2019**, 67(4), 2405-2412.
6. P. Liu, X. Zhu, Y. Zhang, X. Wang, C. Yang, and Z. H. Jiang. Patch antenna loaded with paired shorting pins and h-shaped slot for 28/38 GHz

- dual-band mimo applications, *IEEE Access*, **2020**, 8, 23705-23712.
7. R. K. Meena, M. K. Dabhade, K. Srivastava, and B. K. Kanaujia. *Antenna design for fifth generation (5g) applications*, Proceedings of the 2019 URSI Asia-Pacific Radio Science Conference (AP-RASC), 2019.
  8. W. Ahmad, A. Ali, and W. T. Khan. *Small form factor PIFA antenna design at 28 GHz for 5G applications*, Proceedings of the 2016 IEEE International Symposium on Antennas and Propagation (APSURSI), 2016.
  9. F. N. M. Redzwan, M. T. Ali, M. M. Tan, and N. F. Miswadi. *Design of tri-band planar inverted F antenna (PIFA) with parasitic elements for UMTS2100, LTE and WiMAX mobile applications*, Proceedings of the 2015 International Conference on Computer, Communications, and Control Technology (I4CT), 2015.
  10. M. K. Ishfaq, T. A. Rahman, H. T. Chattha and M. U. Rehman. Multiband split-ring resonator based planar inverted-F antenna for 5G applications, *International Journal of Antennas and Propagation*, **2017**, 5148083.
  11. A. Iftikhar, M. N. Rafiq, M. M. Masud, B. Ijaz, S. Roy and B. D. Braaten. *A dual-band balanced planar inverted F antenna (PIFA) for mobile applications*, Proceedings of the 2013 IEEE Antennas and Propagation Society International Symposium (APSURSI), 2013.
  12. M. Anouar and S. Larbi. *A new PIFA antenna for future mobile and wireless communication*, E3S Web of Conferences, **2022**, 351, 01085.
  13. S. M. A. Ali. An on-chip planar inverted-F antenna at 38 GHz for 5G communication applications, *International Journal of Antennas and Propagation*, **2022**, 1017816.
  14. Y. A. Hashem, O. M. Haraz, and E. D. M. El-Sayed. *6-Element 28/38 GHz dual-band MIMO PIFA for future 5G cellular systems*, Proceedings of the 2016 IEEE International Symposium on Antennas and Propagation (APSURSI), 2016.
  15. T. A. Milligan. Modern antenna design (2<sup>nd</sup> ed.), John Wiley & Sons Inc, New York, 2005.
  16. M. E. Halaoui, L. Canale, A. Asselman, and G. Zissis. *Dual-Band 28/38 GHz Inverted-F Array Antenna for Fifth Generation Mobile Applications*, Multidisciplinary Digital Publishing Institute Proceedings, 2020.